

Density functional study of alkali metal atoms and monolayers on graphite (0001)

K. Rytkönen, J. Akola, and M. Manninen

Nanoscience Center, Department of Physics,

P.O. Box 35, FI-40014 University of Jyväskylä, Finland

(Dated: September 9, 2021)

Abstract

Alkali metal atoms (Li, Na, K, Rb, Cs), dimers and (2×2) monolayers on a graphite (0001) surface have been studied using density functional theory, pseudopotentials, and a periodic substrate. The adatoms bind at the hollow site (graphite hexagon), with Li lying closest to (1.84 Å) and Cs farthest (3.75 Å) from the surface. The adsorption energies range between 0.55 – 1.21 eV, and the energy ordering of the alkali adatoms is $\text{Li} > \text{Cs} \geq \text{Rb} \geq \text{K} > \text{Na}$. The small diffusion barriers (0.02-0.21 eV for the C-C bridge) decrease as the atom size increases, indicating a flat potential energy surface. The formation (cohesion) energies of (2×2) monolayers range between 0.55-0.81 eV, where K has the largest value, and increased coverage weakens the adsorbate-substrate interaction (decoupling) while a two-dimensional metallic film is formed. Analysis of the charge density redistribution upon adsorption shows that the alkali metal adatoms donate a charge of 0.4 – 0.5 e to graphite, and the corresponding values for (2×2) monolayers are $\sim 0.1e$ per atom. The transferred charge resides mostly in the π -bands (atomic p_z -orbitals) of the outermost graphene layer.

I. INTRODUCTION

The adsorption of alkali metals on a graphite surface (highly oriented pyrolytic graphite, HOPG) is widely studied for several reasons. Firstly, adsorbed alkali metal adatoms (dispersed phase) have shown a substantial activity in gasification reactions (catalysis),^{1,2,3} and improved hydrogen physisorption on graphitic hosts (HOPG, carbon nanotubes) has been suggested.⁴ Secondly, alkali metal monolayers (MLs) exhibit interesting metallic properties as they appear as nearly ideal two-dimensional (2D) quantum wells, in which the metal valence electrons are confined and form discrete quantum well states.^{5,6,7,8} Thirdly, most alkali metal adatoms intercalate readily between graphene (GR) layers, and technological applications of lithium-graphite intercalation compounds have been introduced as rechargeable solid-state Li-ion batteries.^{9,10,11,12}

Alkali metals show intriguing structural phase transitions on HOPG, and - despite the similarities in their electronic structure - they exhibit different properties as the adsorbate coverage is increased. A common feature is the formation at low densities of a dispersed and highly polarized phase with a maximal adatom-adatom distance (“correlated liquid”). As the adatom coverage is increased a critical density is obtained, after which a nucleation to more closely packed configurations (islands) occurs.^{13,14} The differences between alkali metals arise in the island formation: Li, for example, forms incommensurate hexagonally close-packed islands on HOPG (provided that it does not intercalate via defects), while K follows a (2×2) construction. The larger alkali metals (Rb and Cs) have been observed to form (2×2) overlayers, and $(\sqrt{3}\times\sqrt{3})R30^\circ$, rotated incommensurate hexagonal $(2\times 2)^*$ as well as $(\sqrt{7}\times\sqrt{7})R19^\circ$ phases have been reported for Cs.^{14,15,16} Sodium is unusual, because its growth scheme changes at 110 K from layer-by-layer to three-dimensional (3D) clustering, and 3ML thick bcc(110) microcrystals with slightly buckled surfaces have been observed.^{5,7} Unlike the other alkali metals, Na also does not form stage 1 intercalation compounds. Only stage 8 compounds have been reported.^{14,17}

The fundamental question of the alkali-HOPG systems concerns the nature of the adsorbate-substrate interaction. It is widely held that the alkali metal donates charge to the substrate π -bands, which dominate the electronic band structure near the Fermi energy (semimetal),^{18,19,20} but the amount of charge transferred is still unclear. Different experimental techniques (electron spectroscopy, work function measurements, photoemission and

photoabsorption) as well as different theoretical approaches (band structure calculations, cluster models) have led to controversial results for the K-HOPG systems. As summarized in the review article by Caragiu and Finberg,¹⁴ the charge transfer in the dispersed phase spans a range of $0.3 - 0.7e$ per adatom, while the decoupled (2×2) islands exhibit values between $0.17 - 0.46e$ per adatom. Experimental studies have focused mainly on the adsorption of potassium, with much less data on the charge transfer for other elements. Theoretical investigations of these systems have focused on Li, Na, and K adatoms,^{3,4,21,22,23,24,25,26,27,28,29,30} while results for the (2×2) coverage have been reported for Li and K.^{3,21,22,25,30}

We report here a systematic density functional study of alkali metal (Li, Na, K, Rb, Cs) adatoms, dimers, and (2×2) monolayers on HOPG. The calculations have been performed using a periodic “slab model” that mimics the real HOPG surface and its electronic band structure, and we use an extensive basis set to describe the subtle adsorbate-substrate interaction accurately. Although other theoretical studies on Li, Na, and K adatoms have been published,^{26,29} our work fills a gap in the theoretical description of alkali metal-HOPG systems. This is a natural extension to our previous study of Na adatoms and clusters on HOPG, where the experimentally observed clustering behavior of Na adatoms was reproduced.²⁷ By applying the same simulation approach to the all alkali metal atoms, we can point out differences between them and seek possible explanations. We report the optimized geometries, energetics, and charge transfer of the alkali-HOPG systems, and provide visualizations of the charge density redistribution (difference) and electron localization function in order to shed light on the adsorbate-substrate interaction. We also discuss the peculiar adsorption properties of Na that appear to be related to its atomic radius and ionization potential.

II. SIMULATION METHODS

The calculations were performed using the Car-Parrinello molecular dynamics program,³¹ which is based on density functional theory (DFT). The electron-ion interaction is described by nonlocal, norm-conserving, and separable pseudopotentials of the form suggested by Troullier and Martins.³² For Li and Na, only the $2s/3s$ valence electron is treated explicitly, while for K, Rb, and Cs we include the semi-core (p-shell) electrons. The program uses periodic boundary conditions and a plane wave basis with a kinetic energy cutoff of 70 Ry. The generalized gradient-corrected approximation of Perdew, Burke and Ernzerhof (PBE) is

adopted for the exchange-correlation energy E_{xc} .³³ The atomic positions are optimized using a quasi-Newton approach (BFGS method)³⁴ until all Cartesian components of the nuclear gradients are below 1×10^{-4} atomic units. The electronic Hamiltonian is re-diagonalized after each optimization step using the Lanczos method, and a finite temperature functional (T = 1000 K) by Alavi *et al.*³⁵ is used for the Kohn-Sham (KS) single-particle state occupancies. This reflects the small energy gap (band gap) between the occupied and unoccupied states of graphite.

The substrate is modeled as a periodic slab of three graphene layers with a stacking *ABA* (Bernal graphite), and it comprises 96 fixed C atoms (32 in each layer). Our previous experience has shown that three GR layers are needed in order to obtain converged results for the alkali atom adsorption if a substantial charge transfer to the substrate occurs.²⁷ The nearest-neighbor C-C distance is 1.421 Å, and the interplanar distance is fixed to the experimental value of 3.354 Å, since the PBE functional used does not describe weak dispersion forces well.³⁶ The model is similar to that used in our earlier work,²⁷ except that the supercell symmetry is hexagonal, not orthorhombic. This is a natural choice for graphite, and it enables us to use fewer \mathbf{k} -points in the simulations. Earlier benchmark tests with an orthorhombic supercell indicated that a $2 \times 2 \times 1$ Monkhorst-Pack \mathbf{k} -point mesh³⁷ is needed to converge the atomic forces, and a $5 \times 5 \times 1$ mesh is required for the energies.²⁷ For the hexagonal supercell symmetry, a $2 \times 2 \times 1$ mesh is adequate for both forces and energy. The lateral dimension of the hexagonal supercell is 9.84 Å, and the perpendicular box size varies between 16.7 – 20.7 Å, depending on the adsorbate (the distance between the replicated slabs is 10 – 14 Å). The maximum lateral separation of the repeated adsorbates is 9.84 Å, and the configuration referred to as a separated adatom corresponds to a (4×4) monolayers.

The effect of the substrate relaxation has been tested in the case of Li adatom by releasing either (a) the six nearest C atoms when Li is above the hollow site (in the middle of a graphite hexagon) or (b) the four nearest C atoms when Li is above the α -site (above a C atom). In the former case, the adatom rises 0.01 Å, and the C atoms move by 0.04 Å. The total energy of the relaxed system is only 0.006 eV lower than for the fixed substrate. In the latter case, Li is lowered by 0.04 Å as the C atoms move 0.01-0.04 Å, and the total energy is reduced by 0.01 eV. The changes will be even less in the other alkali metals, where the binding is weaker.

Our previous investigations of Na-HOPG systems²⁷ indicated that one must use an exten-

sive plane wave basis set in order to describe the subtle charge transfer and redistribution. We showed that the reduction in the cutoff from 70 Ry to 50 Ry led to a 33% (0.17 eV) weaker binding for Na and 7.8% (0.19 Å) larger distance from the surface. The choice of E_{xc} functional is also important, because both the local density (LDA) and gradient-corrected (GGA) approximations do not describe dispersion forces reliably. While LDA often yields overbinding for the metal-adsorbate interaction, GGA methods display the lack of dispersion forces at a large separation between the graphite layers. A benchmark calculation for a Li·C₆H₆ complex results in values 0.22 eV (binding energy) and 2.03 Å (Li separation from the center of the benzene ring), whereas the corresponding second-order Møller-Plesset (MP2) results are 0.25 eV and 2.25 Å.³⁸ A DFT study by Valencia *et al.* reported values 0.71/0.21 eV and 1.65/1.90 Å for L(S)DA/PBE functionals which emphasize the overbinding character of LDA. Furthermore, we have performed another benchmark calculation for K⁺·C₆H₆ in order to test a system with a cation/ π interaction.³⁹ The results for the K⁺ binding energy and distance are 1.04 eV and 2.96 Å, respectively, compared to the MP2 results 0.74 eV and 2.81 Å.⁴⁰ The experimental binding energy (0.83 eV)⁴¹ suggests that PBE slightly overbinds systems with pure cation/ π interaction. We note, however, that the interaction in alkali-benzene systems differs from that on HOPG.

III. RESULTS

The results for the alkali metal adatoms, dimers, and (2×2) monolayers on HOPG are presented in Table I. The formation (cohesion) energy (ΔE), defined as the energy difference between the system and its constituents (separated metal atoms and substrate), comprises the adsorption energy (ΔE_{\perp}) and the binding energy (E_b) of a separated adsorbate (per atom). The potential energy surface of a single alkali adatom (Li, Na, K, Rb, Cs) has been mapped by optimizing the distance from the graphite (0001) surface at four locations: above the hollow site (hexagon center), above the α and β sites (carbons), and above the bridge site (C-C bond). For each alkali adatom, the hollow site is favored energetically, and the optimal diffusion path from one minimum to another one is via the bridge site. The corresponding diffusion barrier height E_{diff} is significantly larger for Li than for the other alkali metals (0.02 – 0.06 eV, see Table I).⁴² These results agree with the findings of Lamoen and Persson, who obtained a maximum variation of 0.05 eV for the K adsorption at different

locations.³ The preference of alkali metals for the hollow site is well known.^{21,23,25,26,43}

Fig. 1 shows the formation and adsorption energies (ΔE and ΔE_{\perp}) as well as the separation from the surface (d_{\perp}) for alkali metal adatoms and (2×2) monolayers (see also Table I). In the case of adatoms, the adsorbate binding energy is negligible, and the adsorption energy is equal to the formation energy. The ΔE values of Li and Na differ, since Li binds relatively strongly to the substrate (1.21 eV), whereas Na has the weakest adsorption (0.55 eV) of all the adatoms. The three larger alkali atoms (K, Rb, Cs) have $\Delta E/\Delta E_{\perp}$ values of the same magnitude (0.99-1.04 eV). For the (2×2) monolayers, the trend in ΔE_{\perp} is similar to that in separated adatoms, with Li and Na providing the upper/lower boundaries (0.39/0.16 eV). The behavior of the formation energies is slightly different, as K forms the most stable (2×2) construction, and ΔE decreases for Rb and Cs. Despite the fact that Li and Na do not form (2×2) monolayers, Li also has a considerable formation energy. Cesium becomes slightly compressed in the 2D graphite mesh (nearest-neighbor distance 4.92 Å compared to 5.24 Å of bulk Cs), causing a lower adsorbate binding energy. The adatoms (especially K) have larger ΔE values than (2×2) monolayers, which supports the experimental observation of the dispersed phase at low adatom coverage.

The surface separation of alkali metal adatoms [Fig. 1(b)] increases as the atomic radius increases, and the d_{\perp} values range between 1.84 – 3.44 Å. For the (2×2) monolayers, d_{\perp} increases systematically as the metal films decouple from the surface, and the corresponding range of values is 2.02 – 3.75 Å. The decoupling effect is reflected in the adsorption energies, which are smaller than for the separated adatoms. The Na (2×2) monolayer is remarkably far from the surface (3.16 Å), illustrating further that this construction is unfavorable. Among the two smallest alkalis, Li appears more able to adjust to the underlying graphite lattice. This is in accordance with the experimentally observed intercalation properties.

An exceptionally weak interaction of Na_2 with HOPG was found in our earlier study,²⁷ and further calculations of both horizontally and vertically aligned dimers show that the adsorption is also weak for the latter orientation (Table I). This indicates that Na_2 is almost decoupled from the surface, and the corresponding formation energy (ΔE) is similar to that of a single adatom. Alkali metal dimers have two valence electrons and a closed-shell electronic structure, and their interaction with HOPG is significantly weaker than for adatoms. Comparison of the dimer bond lengths (R_{dim}) shows that Li_2 and K_2 elongate (10-15%) upon binding with HOPG, with a smaller effect in Na_2 .

In the case of two K (2×2) overlayers, ΔE_{\perp} is approximately one half of the corresponding value for one ML (Table I), but the total adsorption energies are close (~ 1.0 eV per substrate area). The surface separation of the lower monolayer ($d_{\perp}=3.11$ Å) is also similar to that for one ML ($d_{\perp}=3.17$ Å), so that the interaction between the K overlayers and HOPG is weak. The experimental value $d_{\perp}=2.79\pm 0.03$ Å for a K (2×2) layer (low-energy electron diffraction, LEED)⁴⁴ is closer to the value ($d_{\perp}=2.72$ Å) obtained for separated K atom (Table I). The separation of the K overlayers is 3.90 Å, and the nearest-neighbor distance between K atoms at different layers is 4.85 Å (within a layer 4.92 Å). The formation energies of 1ML and 2ML systems are similar, and we conclude that K atoms bind with 0.8-1.0 eV on HOPG. The desorption kinetics model by Lou *et al.* that is fitted to experimental data yields a desorption energy of 1.0 eV.²³

Our calculations of alkali metal adsorption are compared with other DFT studies in Table II. We have included results for Li, Na, and K, but we found no theoretical studies of larger alkali metal atoms on graphite. The range of adatom cohesion energies is 1.10 – 1.68 eV for Li, 0.50 – 0.72 eV for Na, and 0.51 – 1.67 eV for K, and our values are near the lower bound for Li and Na. For K we obtain ΔE that is in the middle of the broad range. The adatom d_{\perp} values show deviations of 0.2 – 0.4 Å, where our results represent the upper boundary for Li and Na. There are two reasons behind the scatter of data: LDA is known to overbind, and the cluster models are not completely representative of HOPG because of their electronic structure (energy gap between the occupied and unoccupied orbitals). Furthermore, the good agreement with the recent study by Valencia *et al.*²⁹ is due to the similar simulation model (slab geometry, PBE functional, plane wave basis). We know of no other calculations of the Na (2×2) monolayer, and the comparison is limited to Li and K. For Li, our results differ significantly from the study by Khantha *et al.*,²⁵ emphasizing the sensitivity to the choice of E_{xc} functional. Benchmark calculations for a Li-C₆H₆ complex have demonstrated that LDA leads to overbinding,²⁹ and we have more confidence in our PBE results. On the other hand, for K (2×2) ML the experimental layer spacing (2.79 Å, LEED)⁴⁴ is closer to the LDA result.

Charge transfer between the adsorbate and substrate has been studied by subtracting the calculated electron densities of HOPG and metal layer from that of the whole system.^{3,21,27} Fig. 2 shows the laterally averaged charge density difference ($\Delta\rho_{\perp}$, z direction) for K, Rb and Cs adatoms and monolayers. In order to obtain reliable $\Delta\rho_{\perp}$ profiles, we have

recalculated the electron densities within a vertically extended simulation box ($c=26.71 \text{ \AA}$). A significant accumulation below the lowermost graphene layer (GR1) was found for Na in our earlier study ($c=18.71 \text{ \AA}$),²⁷ and we confirm that this is a finite size effect caused by the dipole-dipole interaction of the periodic systems.²⁹ Our benchmark calculation show that this undesirable effect of periodicity is reduced as the perpendicular distance between the slabs is increased up to 20 \AA .

Fig. 2 shows that charge is depleted mainly from the adsorbate and accumulated in the vicinity of the topmost graphene layer (GR3). There is also a small accumulation on both sides of the lower graphene layers (GR1 and GR2), and a small depletion within the layers. There are only small qualitative differences between the three largest alkali metals: the location and width of the charge depletion node (alkali metal) depends on the atomic radius, and K has the most pronounced accumulation above GR3. Within the substrate range, the $\Delta\rho_{\perp}$ curves are identical. For the (2×2) MLs, the curves resemble closely each other, again, with minor deviations near the adsorbate planes. The $\Delta\rho_{\perp}$ variations are larger for MLs compared to adatoms, and the weight of GR2 is slightly enhanced.

A layer-by-layer analysis of the charge transfer in the alkali-HOPG systems is given in Table III. Also shown is the adsorbate-substrate cutoff distance (R_{cut}), which defines where the charge accumulation changes to depletion above the substrate. This distance is relatively insensitive to the atomic radius of the alkali metal atom, and for adatoms its values range from 1.67 \AA (Li) to 1.79 \AA (Cs). The situation changes little for the (2×2) monolayers (Li and Cs 1.48 and 1.63 \AA , respectively), but there is a systematic shift downwards. The charge transfer is calculated by integrating $\Delta\rho_{\perp}$ over a range of z -values, and corresponds for a metal adsorbate to the negative node (depletion area) around the alkali metal layer. With small ionic radii and large ionization potentials (IP), Li and Na donate small amounts of charge ($\Delta q \sim -0.4e$), while the other adatoms show a depletion of ~ 0.5 electrons. The charge transfer changes little when the coverage is increased from a (4×4) monolayer (separated adatom) to a (2×2) monolayer. The charge transfer from individual adsorbate atoms then decreases as the alkali coverage increases, in accordance with the calculated adsorption energies (Table I). The largest change is observed for Na, where Δq changes from -0.44 to $-0.34e$ ($-0.09e$ per adatom) upon increasing the coverage. This is further evidence of the unusually strong decoupling of Na. Furthermore, inspection of the individual GR layers shows that the largest charge accumulation occurs in the topmost layer (GR3),

and the net contribution of the two lower layers (GR1 and GR2) ranges between 29-45%.

The charge density difference ($\Delta\rho$) and electron localization function (ELF)⁴⁵ of Li (2×2) ML on HOPG are shown in Fig. 3. This is not a stable monolayer, as Li tends to form hexagonal incommensurate structures (if it does not intercalate), but it serves to visualize the Li-HOPG interaction. Each Li atom donates charge to the six nearest C atoms [Fig. 3(a)], and the underlying hexagonal symmetry is reflected in the shape of the charge accumulation lobes. Other areas of charge accumulation [Fig. 3(b), red color] can be seen above the Li atoms and above and below the C atoms of GR2. Charge depletion (blue color) is visible in the Li layer, and especially between the Li atoms. The topmost graphene layer also shows significant depletion. The electron localization function [ELF, Fig. 3(c)] reflects the probability of finding two electrons at the same location, and it ranges from 0 (no localization, blue) to 1 (complete localization, red). A reference value of 0.5 (green color) corresponds to a homogeneous electron gas (metallic bonding), and covalent bonds appear red due to the electron pairing (see C-C bonds). The ELF shows no electron overlap within the Li ML, indicating weak chemical bonding between the Li atoms, and the very low electron density within the Li plane is consistent with the small value of ELF. This is reflected also in the adsorbate-substrate interface, and the lack of electron overlap suggest that there are no Li-C bonds present. However, the ELF contours of the nearest C-C bonds deform towards Li, which can be regarded as a sign of polarization (induction) that is an important component in the cation/ π interaction.⁴⁰ Finally, charge redistribution results in a 'cap' of localized electron density above each Li atom.

The laterally averaged charge density difference ($\Delta\rho_{\perp}$) curves for a separated K adatom, a (2×2) monolayer, and two (2×2) overlayers on HOPG are shown in Fig. 4. Table III shows that there is a charge transfer from the metal film towards HOPG: $\Delta q = -0.53e$ for a separated K atom, $-0.50e$ for K (2×2) ML, and $-0.48e$ for two K (2×2) layers. Decoupling causes visible differences: the charge is depleted from the K adatom, whereas in the cases of (2×2) overlayers depletion is mainly beneath the lower K layer. The curves for 1ML and 2ML below the adsorbate are almost identical, the charge transfer per K atom in the adsorbate-substrate interface is slightly smaller for 2ML ($-0.12e$) than for 1ML ($-0.13e$), and there is a small accumulation between the K layers. Similar analyses of $\Delta\rho_{\perp}$ in other DFT calculations have given Δq values ranging between -0.38 and $-0.46e$ for K,^{3,21,29} and $-0.17e$ for (2×2) ML.^{3,21}

The charge density difference and ELF of two K (2×2) overlayers on HOPG are given in Fig. 5. Charge accumulates mainly above the C atoms of the topmost GR layer [Figs. 5(a) and 5(b)], and other regions can be seen above and below the C atoms of GR1 and GR2, and in the vicinity of K atoms. Depletion occurs mainly below the lower K layer and in the C-C bonds of GR3. Furthermore, a trace of depletion (light blue color) can be observed above the topmost K layer. These findings lead to a picture where the alkali metal donates charge to the π -bands (atomic p_z -orbitals) of the GR planes, and there is depletion in the sp^2 hybridized σ -bands of the topmost GR layer. The electron localization function [Figs. 5(c) and 5(d)] shows that the electron density is delocalized (~ 0.5) between the K atoms, so that K forms a metallic layer on HOPG. The boundary between the metal film and 'vacuum' is sharp and flat, and this is confirmed by the electron density contours (not shown). This picture agrees with the He-scattering experiments for alkali (2×2) layers, where no corrugation was found in the surface potential.²² The blue rings around the individual K atoms show that it is extremely unlikely to find more than one electron within a range of the K $4s$ orbital (notice the localized $3p$ electrons). ELF shows that there is no chemical bonding between the adsorbate and substrate, as the interface region appears in blue color (delocalization). This indicates that the adsorbate-substrate interaction should be viewed as ionic.

The electronic density of states (DOS) of two K (2×2) overlayers on HOPG as well as the DOS of the separated subsystems are shown in Fig. 6. The calculations were performed with a $13\times 13\times 1$ Monkhorst-Pack \mathbf{k} -point mesh corresponding to 87 explicit \mathbf{k} -points in the lateral dimension. The graphite DOS (lower panel) shows typical features: a steep rise at -20 eV due to the 2D character of graphite, a dip at -13 eV after the first two σ bands, a large peak at -6.5 eV followed by a shoulder, and a zero weight and zero gap at the Fermi energy.^{18,19,27} Despite the charge transfer and redistribution, the characteristic features of the graphite DOS remain as the K film is added (upper panel). The sharp peak at -16 eV corresponds to the K $3p$ semicore electrons, and important changes are seen near the Fermi energy, where the system shows a deviation from the "V shaped" profile of HOPG. The DOS of the separated K film (lower panel, dashed line) shows terrace-like features in agreement with a free-electron model for a 2D metal, and it has a finite weight at the Fermi energy (second terrace). The DOS of the whole system can then be understood as a sum of its constituents, where K forms a decoupled metallic layer that has signs of quantization in the

perpendicular direction.

Recent photoemission experiments and DFT calculations of Pivetta *et al.* reported that the adsorption of alkali atoms induces a gap opening in the surface electronic structure of HOPG,²⁸ and the calculated DOS for a Na adatom [(5×5) construction, three GR layers] showed a gap of 0.15 eV in DOS. This is 0.4 eV below the Fermi level and in very good agreement with experiment. It was suggested that the origin of this feature lies in the charge transfer to the topmost GR layers (each is a 2D semimetal and accepts varying amounts of charge), and this causes perturbations in the graphite electronic band structure. We have analyzed the electronic band structure of Na adatom on HOPG (not shown) and find a similar gap (0.17 eV) at -0.55 eV. The slight difference between the numerical values is probably due to the different coverage [(4×4) construction in the present work].

IV. CONCLUSION

We have made a systematic study of alkali metal atoms, dimers and monolayers on HOPG using a DFT method employing a periodic slab geometry (\mathbf{k} -points) and an extensive plane wave basis set. This method enables us to capture the band structure of graphite and model a real substrate, unlike other that use a "cluster model". Our previous experience with Na clusters on HOPG²⁷ has shown that a large basis set and a substrate of three GR layers are needed in order to describe the details of adsorbate-substrate interaction accurately. The calculations are demanding in terms of both CPU time and memory.

In order to simulate separated adatoms, a (4×4) coverage has been chosen (adatom separation 9.84 Å), resulting in a model substrate of 32 C atoms per GR layer (altogether 96 C atoms). This coverage is still far from the "real" dispersed phase with alkali-alkali distances of several nanometers, where the interaction is dominated by the Coulomb interaction with the positively charged adatoms, and we expect a slight shift in the adatom adsorption energies as the coverage is decreased. The same model substrate has been applied for the other adsorbates as well, in order to permit a detailed comparison with the calculated numerical values. The bond lengths of Rb and Cs dimers were too large for the lateral dimension of the simulation box, and they were not considered in this study.

In general, alkali metal adatoms bind at the hollow site of the hexagonal graphite surface with adsorption energies ranging between 0.55 – 1.21 eV. The ordering of binding energies is

Li>Cs \geq Rb \geq K>Na, and the weak binding of Na compared with Li and K has been reported by earlier studies.^{26,29} The mapping of the adatom locations on HOPG shows that Li has a moderate diffusion barrier of 0.21 eV, whereas the larger alkalis are relatively mobile with diffusion barriers of 0.02 – 0.06 eV. The results for the (2 \times 2) monolayers show that the "dispersed" phase is more stable except for Na. This result is particularly important for the larger alkalis (K, Rb, Cs), which form (2 \times 2) MLs as the coverage increases above a certain critical value.¹⁴ The ordering K>Rb>Cs does not conform to the bulk nearest-neighbor distances, where Rb has the closest value of 4.84 Å compared with the monolayer value (4.92 Å, note the change from 3D to 2D). The low formation energy of Cs may be due to the compressed Cs-Cs bonds, since the bulk nearest-neighbor distance is 5.24 Å. Despite the pronounced decoupling from the surface, Na monolayer has a comparable formation energy to the adatom case, which is consistent with the clustering processes found experimentally and theoretically.^{5,7,27}

The amount of charge transfer and the nature of the alkali-HOPG interaction have been subjects of debate for many years. Our systematic study of the electron density redistribution upon adsorption ($\Delta\rho_{\perp}$) suggests that the charge loss is 0.4 – 0.5 e per alkali adatom. Furthermore, values of the order of 0.1 e per atom have been observed for (2 \times 2) MLs, indicating a decoupling effect between the alkali layer and HOPG. The analysis of the charge density redistribution in the substrate shows that the accepted charge resides mainly in the topmost graphene layer. We note that the calculated Δq values depend on the method of evaluation, as recently shown by Valencia *et al.* for several approaches ($\Delta\rho_{\perp}$, Löwdin charge analysis, Bader atoms, Voronoi deformation charge).²⁹ We prefer the simplicity of a method based on $\Delta\rho_{\perp}$, which can be used for different alkali metals without adjustable parameters.

The visualizations of the Li and K overlayers shed light to the alkali-HOPG interaction. In the case of two K (2 \times 2) MLs, K forms a metallic film that donates charge to the π -bands of the substrate. The corresponding region of charge depletion is restricted to below the metal layer, and ELF further validates the picture of a decoupled 2D metal (ionic bonding). The situation is slightly different for Li (2 \times 2) ML, as there is a pronounced charge accumulation towards the six nearby C atoms, and the Li atoms appear more localized. This is to be expected, because the Li-Li separation is far from that in bulk (3.04 Å). ELF indicates that there is no chemical bonding between the adsorbate and HOPG, but a trace of polarization can be observed in the nearby C atoms.

Finally, we turn to an obvious question raised by this article: Why does Na bind the weakest among all the alkali metals? The quantum chemical calculations of cation/ π complexes by Tsuzuki *et al.*⁴⁰ showed that polarization (induction) and electrostatic interactions are the major sources of attraction, and the polarization dominates binding with Li^+ and Na^+ . Furthermore, the polarization energy was estimated to be proportional to R^{-4} for cation-benzene complexes (R is the separation from the center of the benzene ring).⁴⁰ If we study the corresponding d_{\perp} values in Table I, we see that the alkali separation is 0.6 Å larger for Na than for Li. On the other hand, the slight decrease in IP (5.39 \rightarrow 5.14 eV) indicates that the cost of transferring charge from the alkali towards HOPG (work function \sim 4.6 eV) is not lowered significantly. A similar comparison between Na and K shows a significant drop in IP (0.8 eV), but a small increase in d_{\perp} . We expect that K binds more strongly than Na, and the high ionization potential and the relatively large surface separation (atomic radius) of Na are then responsible for the weak binding on graphite.

V. ACKNOWLEDGMENTS

Financial support from the Academy of Finland and from the European Community project ULTRA-1D (NMP4-CT-2003-505457) is acknowledged. The calculations were performed on IBM-SP4(+) computers at the Center for Scientific Computing (CSC), Espoo, Finland, and at the John von Neumann Institute for Computing (NIC), Forschungszentrum Jülich, Germany. We thank R.O. Jones for a critical reading of the manuscript.

¹ K.M. Hock, J.C. Barnard, R.E. Palmer, and H. Ishida, Phys. Rev. Lett. **71**, 641 (1993).

² C. Janiak, R. Hoffmann, P. Sjövall, and B. Kasemo, Langmuir **9**, 3427 (1993).

³ D. Lamoén and B.N.J. Persson, J. Chem. Phys. **108**, 3332 (1998).

⁴ I. Cabria, M.J. López, and J.A. Alonso, J. Chem. Phys. **123**, 204721 (2005)

⁵ M. Breitholtz, T. Kihlgren, S.-Å. Lindgren, H. Olin, E. Wahlström, and L. Walldén, Phys. Rev. B **64**, 073301 (2001).

⁶ M. Breitholtz, T. Kihlgren, S.-Å. Lindgren, and L. Walldén, Phys. Rev. B **66**, 153401 (2002).

⁷ M. Breitholtz, T. Kihlgren, S.-Å. Lindgren, and L. Walldén, Phys. Rev. B **67**, 235416 (2003).

- ⁸ J. Algdal, M. Breitholtz, T. Kihlgren, S.-Å. Lindgren, and L. Walldén, *Phys. Rev. B* **73**, 165409 (2006).
- ⁹ M.S. Dresselhaus and G. Dresselhaus, *Adv. Phys.* **30**, 139 (1981).
- ¹⁰ B. Jungblut and E. Hoinkis, *Phys. Rev. B* **40**, 10810 (1989).
- ¹¹ Z. P. Hu and A. Ignatiev, *Phys. Rev. B* **30**, 4856 (1984).
- ¹² J.-M. Tarascon and M. Armand, *Nature* **414**, 359 (2001).
- ¹³ M.R.C. Hunt and R.E. Palmer, *Phil. Trans. R. Soc. Lond. A* **356**, 231 (1998).
- ¹⁴ M. Caragiu, and S. Finberg, *J. Phys.: Condens. Matter* **17**, R995 (2005).
- ¹⁵ Z.P. Hu, N.J. Wu and A. Ignatiev, *Phys. Rev. B* **33**, 7683 (1986).
- ¹⁶ M.R.C. Hunt, P.J. Durston, and R.E. Palmer, *Surf. Sci.* **364**, 266 (1996).
- ¹⁷ M.T. Johnson, H.I. Starnberg, and H.P. Hughes, *Surf. Sci.* **178**, 290 (1986).
- ¹⁸ J.-C. Charlier, X. Gonze, and J.-P. Michenaud, *Phys. Rev. B* **43**, 4579 (1991).
- ¹⁹ J.-C. Charlier, J.-P. Michenaud, and X. Gonze, *Phys. Rev. B* **46**, 4531 (1992).
- ²⁰ J.C. Boettger, *Phys. Rev. B* **55**, 11202 (1997).
- ²¹ F. Ancilotto and F. Toigo, *Phys. Rev. B* **47**, 13713 (1993).
- ²² J.D. White, J. Cui, M. Strauss, R.D. Diehl, F. Ancilotto, and F. Toigo, *Surf. Sci.* **307-309**, 1134 (1994).
- ²³ L. Lou, L. Österlund, and B. Hellsing, *J. Chem. Phys.* **112**, 4788 (2000).
- ²⁴ J.-F. Gal, P.-C. Maria, M. Decouzon, O. Mó, M. Yáñez, and J.L.M. Abboud, *J. Am. Chem. Soc.* **125**, 10394 (2003).
- ²⁵ M. Khantha, N.A. Cordero, L.M. Molina, J.A. Alonso, and L.A. Girifalco, *Phys. Rev. B* **70**, 125422 (2004).
- ²⁶ Z.H. Zhu, G.Q. Lu, *Langmuir* **20**, 10751 (2004).
- ²⁷ K. Rytönen, J. Akola, and M. Manninen, *Phys. Rev. B* **69**, 205404 (2004).
- ²⁸ M. Pivetta, F. Patthey, I. Barke, H. Hövel, B. Delley, and W.-D. Schneider, *Phys. Rev. B* **71**, 165430 (2005).
- ²⁹ F. Valencia, A.H. Romero, F. Ancilotto, and P.L. Silvestrelli, *J. Phys. Chem. B* **110**, 14832 (2006).
- ³⁰ O. Hjortstam, J.M. Wills, B. Johansson, and O. Eriksson, *Phys. Rev. B* **58**, 13191 (1998).
- ³¹ CPMD V3.9 Copyright IBM Corp 1990-2005, Copyright MPI für Festkörperforschung Stuttgart 1997-2001.

- ³² N. Troullier and J.L. Martins, Phys. Rev. B **43**, 1993 (1991).
- ³³ J.P. Perdew, K. Burke, and M. Ernzerhof, Phys. Rev. Lett. **77**,3865 (1996).
- ³⁴ R. Fletcher, *Practical methods of Optimization* (Wiley, New York, 1980), Vol. 1.
- ³⁵ A. Alavi, J. Kohanoff, M. Parrinello, and D. Frenkel, Phys. Rev. Lett. **73**, 2599 (1994).
- ³⁶ K.R. Kganyago and P.E. Ngoepe, Phys. Rev. B **68**, 205111 (2003).
- ³⁷ H.J. Monkhorst and J.D. Pack, Phys. Rev. B **13**, 5188 (1976).
- ³⁸ J.M. Vollmer, A.K. Kandalam, and L.A. Curtiss, J. Phys. Chem. A **106**, 9533 (2002).
- ³⁹ J.C. Ma and D.A. Dougherty, Chem. Rev. **97**, 1303 (1997).
- ⁴⁰ S. Tsuzuki, M. Yoshida, T. Uchimaru, and M. Mikami, J. Phys. Chem. A **105**, 769 (2001).
- ⁴¹ J. Sunner, K. Nishizawa, P. Kebarle, J. Phys. Chem. **85**, 1814 (1981).
- ⁴² The energy difference between the potential energy maximum (above C atoms) and the saddle point (C-C bridge) is 0.03 eV for Li, and less than 0.01 eV for the other alkali metals.
- ⁴³ Z.H. Zhu, G.Q. Lu, and F. Y. Wang, J. Phys. Chem. B *109*, 7923 (2005).
- ⁴⁴ N. Ferralis, K. Pussi, S. E. Finberg, J. Smerdon, M. Lindroos, R. McGrath, and R. Diehl, Phys. Rev. B **70**, 245407 (2004).
- ⁴⁵ See, for example, A. Savin, R. Nesper, S. Wengert, and T.F. Fässler, Angew. Chem. Int. Ed. **36**, 1808 (1997).

Figures

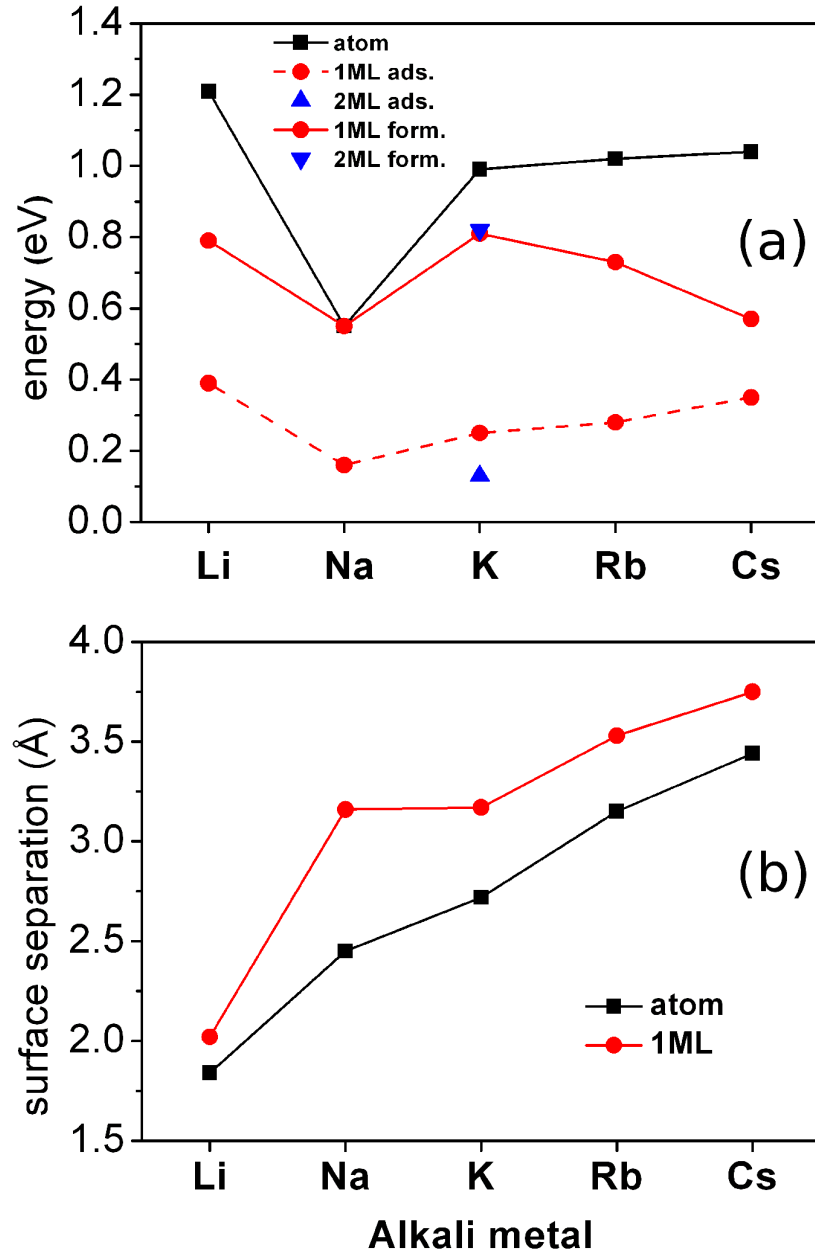


FIG. 1: Adsorption of alkali metal atoms and (2×2) monolayers on HOPG: (a) the formation and adsorption energies per atom (ΔE and ΔE_{\perp}), and (b) the vertical separation from the substrate (d_{\perp}).

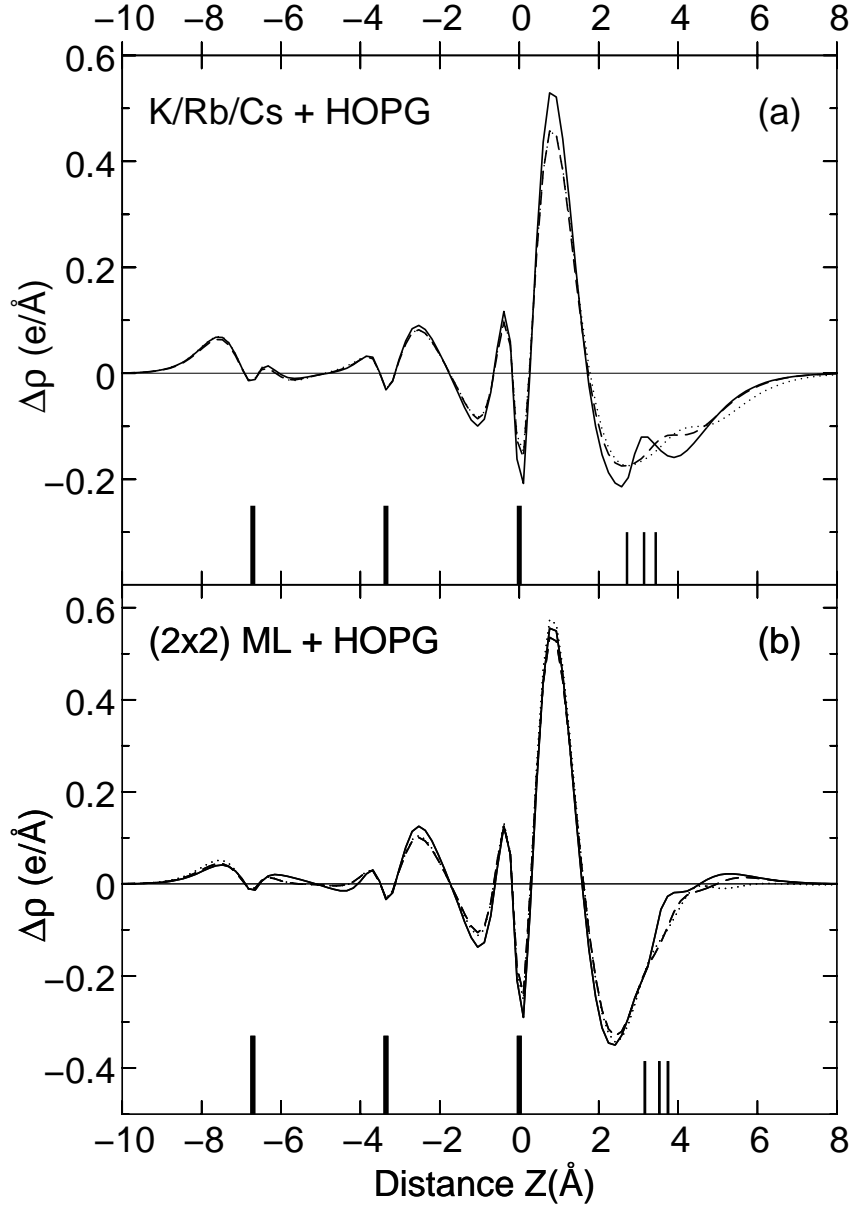


FIG. 2: Laterally averaged charge density difference ($\Delta\rho_{\perp}$, z direction) of K (solid curve), Rb (dashed curve), and Cs (dotted curve) adatoms as well as (2×2) monolayers on graphite. (a) Separated adatoms, and (b) (2×2) monolayers. The vertical bars denote the positions of GR layers (thick bars) and alkali metal (thin bars). The charge densities have been calculated in an extended simulation box, so that the distance between the vertically repeated substrates is 20 \AA . Notice the different scale of $\Delta\rho_{\perp}$ in (a) and (b).

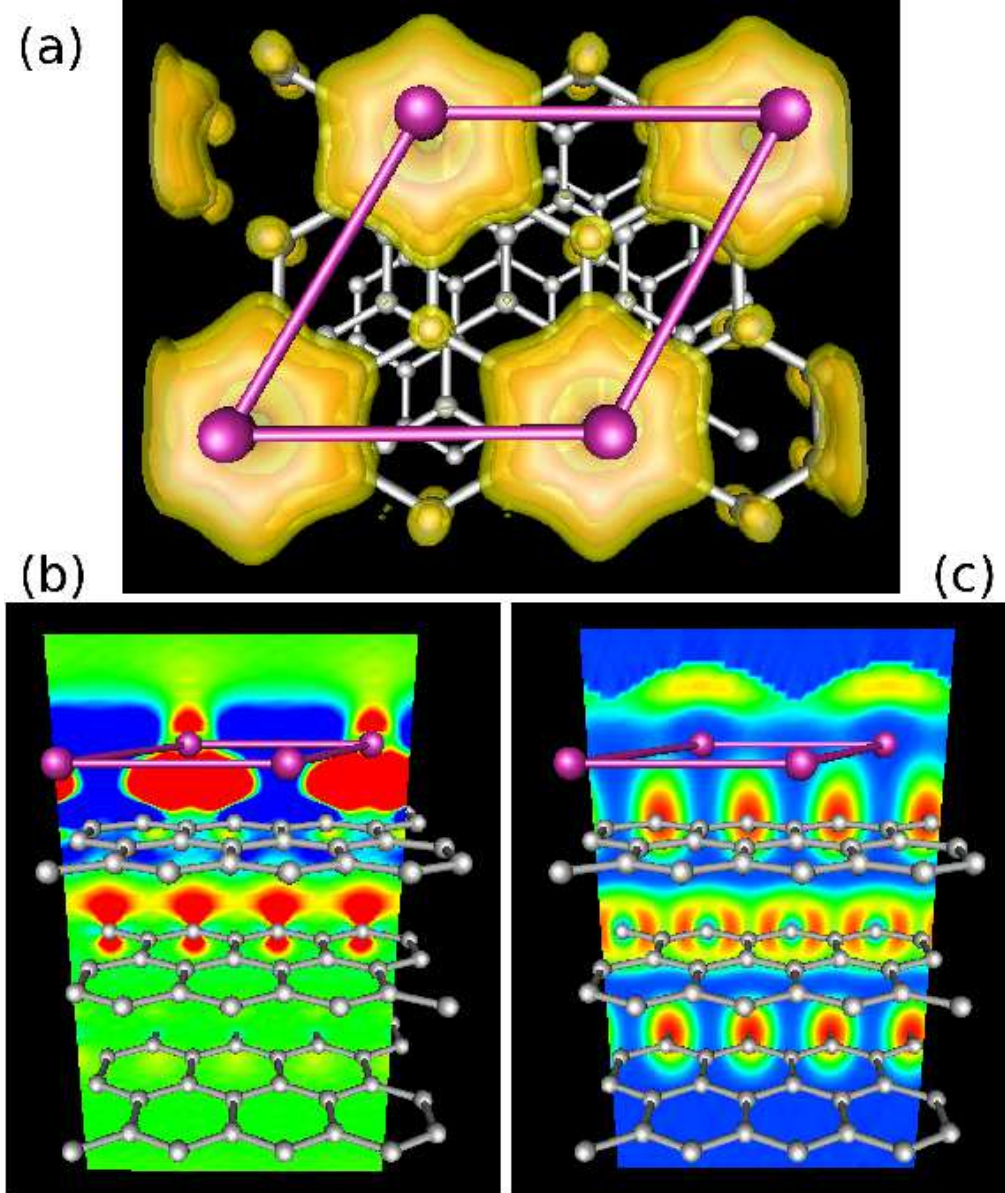


FIG. 3: Visualization of the Li (2×2) monolayer on HOPG. (a) Three isosurfaces for the accumulated electron density. The corresponding values are 0.001 (yellow), 0.002 (orange), and $0.004e/\text{\AA}^3$ (red), respectively. The Li atoms are marked by magenta spheres. (b) Cutplane presentation of the charge density difference (xz plane), where the red color corresponds to accumulation ($0.0005e/\text{\AA}^3$ or more) and blue depletion ($-0.0005e/\text{\AA}^3$ or less). (c) The electron localization function (ELF, xz plane), where the red color corresponds to full localization (1.0, covalent bonds), green is analogous to homogeneous electron gas (0.5, metallic bonding), and blue equals to low localization (0.0).

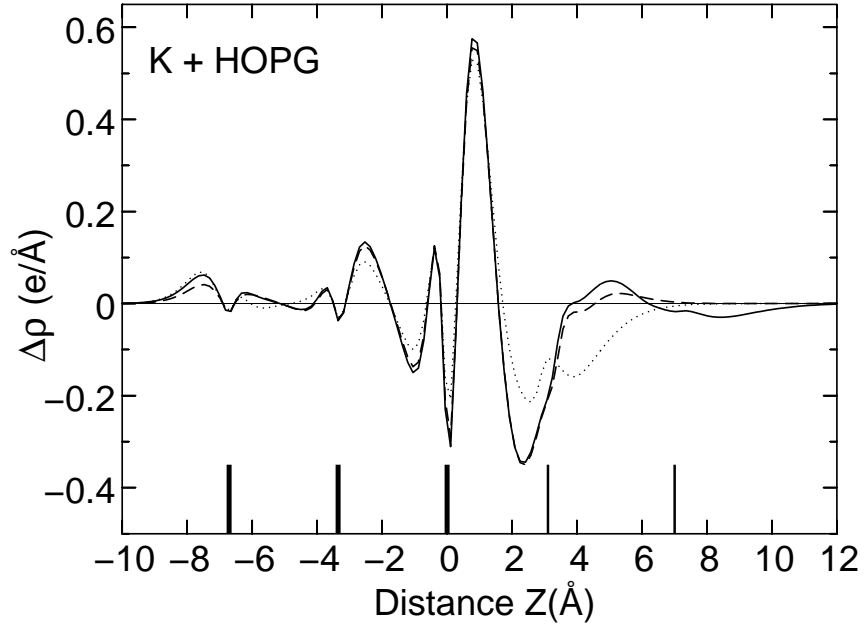


FIG. 4: Laterally averaged charge density difference ($\Delta\rho_{\perp}$) of a K adatom (solid curve), a (2×2) monolayer (dashed curve), and two (2×2) overlayers (dotted curve) on graphite. The vertical bars denote the positions of GR (thick bars) and K layers (thin bars, 2ML). The charge densities have been calculated in an extended simulation box, so that the distance between the vertically repeated substrates is 20 Å.

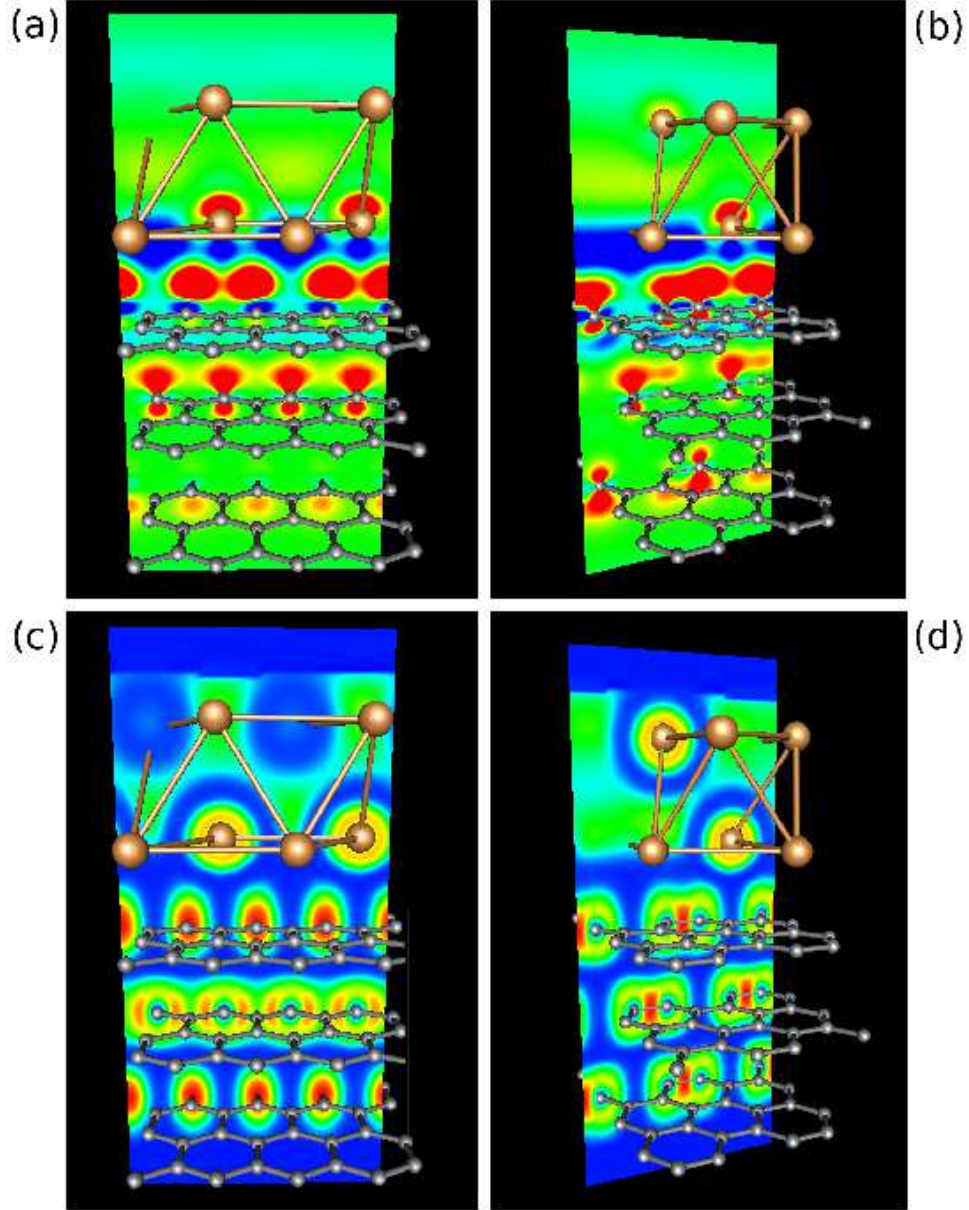


FIG. 5: Cutplane visualization of two K (2×2) overlayers on HOPG. (a-b) The charge density difference is presented in xz and yz planes, where the red color corresponds to accumulation ($0.0005e/\text{\AA}^3$ or more) and blue depletion ($-0.0005e/\text{\AA}^3$ or less). (c-d) Similar presentation of ELF (see the caption in Fig. 3).

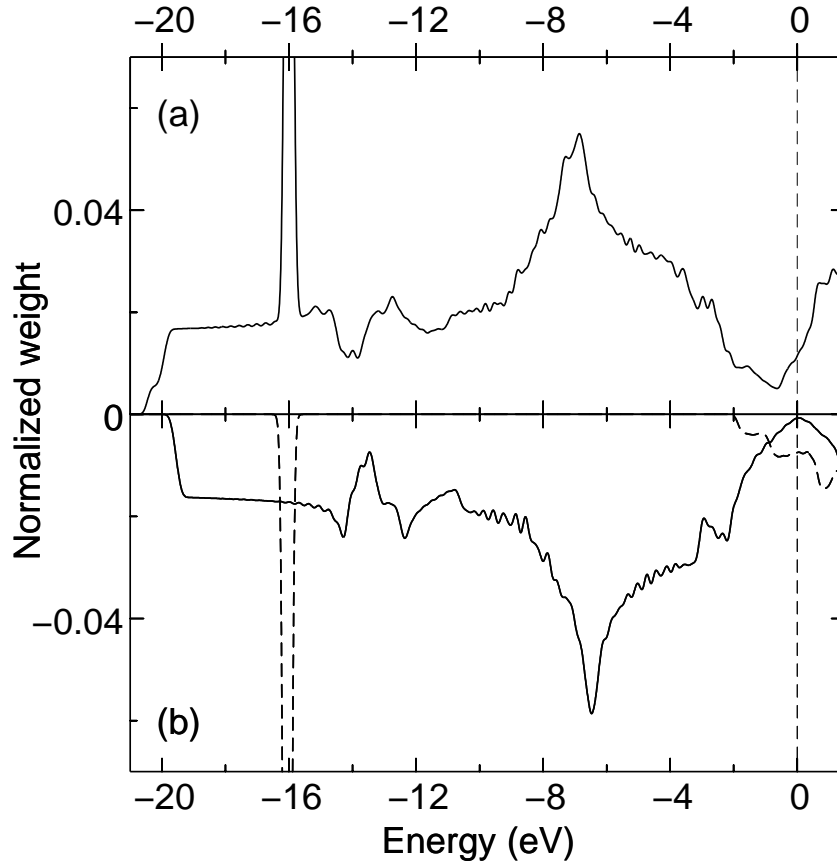


FIG. 6: Normalized density of states (DOS) of (a) two K (2×2) overlayers on HOPG, and (b) the separated substrate (solid line) and K film (dashed line). The energy bands are calculated with a $13\times 13\times 1$ \mathbf{k} -point mesh, and Gaussians of 0.10 eV width were used for each data point. The vertical dashed line marks the Fermi energy.

Tables

TABLE I: Alkali metal atoms, dimers, and (2×2) monolayers on graphite (0001). The formation energy per atom (ΔE) consists of the adsorption energy (ΔE_{\perp}) and adsorbate binding energy (E_b). The diffusion barrier (E_{diff}) corresponds to a C-C bridge location as the adatoms prefer the hollow site. The vertical displacement from the uppermost graphene plane (d_{\perp}), the bond distance of alkali dimers (R_{dim}), and the estimated charge transfer (Δq) are reported also. $\Delta q < 0$ implies a charge transfer to the substrate (in electrons/ $9.84 \times 8.53 \text{ \AA}^2$).

Adsorbate	ΔE (eV)	ΔE_{\perp} (eV)	E_b (eV)	E_{diff} (eV)	d_{\perp} (\AA)	R_{dim} (\AA)	Δq
Li atom	1.21	1.21	-	0.21	1.84	-	-0.42
Li ₂ [†]	0.89/0.81	0.40/0.33	0.50	-	2.03/2.07	2.95/2.90	-
						(2.68)	
(2×2) ML	0.79	0.39	0.40	-	2.02	-	-0.42
Na atom	0.55	0.55	-	0.06 [‡]	2.45	-	-0.44
Na ₂ ^{†,‡}	0.49/0.55	0.14/0.20	0.35	-	3.95/3.05	3.07/3.16	-
						(3.05)	
(2×2) ML	0.55	0.16	0.40	-	3.16	-	-0.34
K atom	0.99	0.99	-	0.05	2.72	-	-0.53
K ₂ [†]	0.74/0.62	0.40/0.28	0.34	-	2.91/2.93	4.65/4.49	-
						(4.04)	
(2×2) ML	0.81	0.25	0.56	-	3.17	-	-0.50
2ML	0.82	0.13	0.68	-	3.11/7.01	-	-0.48
Rb atom	1.02	1.02	-	0.03	3.15	-	-0.48
(2×2) ML	0.73	0.28	0.46	-	3.53	-	-0.48
Cs atom	1.04	1.04	-	0.02	3.44	-	-0.50
(2×2) ML	0.57	0.35	0.22	-	3.75	-	-0.52

[†]The first value is for the horizontal and the second for the vertical orientation of a dimer. The number in parentheses is the gas phase value.

[‡]Calculated in an orthorhombic box. The geometry optimization is done with the $2 \times 2 \times 1$ \mathbf{k} -point

mesh, and the energy is calculated with the $5 \times 5 \times 1$ \mathbf{k} -point mesh.

TABLE II: Comparison between different DFT methods.

Adsorbate	Functional	ΔE (eV)	d_{\perp} (Å)	Reference	
Li atom	PBE	1.21	1.84	This work	
	PBE (LDA)	1.10 (1.68)	1.71 (1.63)	Ref. 29, slab model	
	B3LYP	1.36	1.71	Ref. 26, cluster model	
	LDA	1.60	1.64	Ref. 25, slab model	
(2×2) ML	PBE	0.79	2.02	This work	
	LDA	0.93	1.64	Ref. 25, slab model	
Na atom	PBE	0.55	2.45	This work	
	PBE	0.50 (0.69)	2.34 (2.42)	Ref. 29, slab model	
	B3LYP	0.72	2.10	Ref. 26, cluster model	
	PW91		2.32	Ref. 28, slab model	
K atom	PBE	0.99	2.72	This work	
	PBE (LDA)	0.88 (1.12)	2.65 (2.70)	Ref. 29, slab model	
	BP86 (LDA)	1.49 (1.67)	2.81 (2.73)	Ref. 23, cluster model	
	B3LYP	1.06	2.51	Ref. 26, cluster model	
	LDA	0.51	2.79	Ref. 3, slab model	
	LDA	0.78	2.77	Ref. 21, slab model (1 GR)	
	(2×2) ML	PBE	0.81	3.17	This work
	LDA	0.98	2.82	Ref. 3, slab model	
LDA	0.48	2.82	Ref. 21, slab model (1 GR)		

TABLE III: Charge transfer within the alkali-HOPG systems (in electrons/ $9.86 \times 8.53 \text{ \AA}^2$). N is the number alkali atoms in the simulation box and R_{cut} is the adsorbate-substrate cutoff distance. The values in parentheses are the charge transfer per alkali metal adatom.

Adsorbate	GR1	GR2	GR3	Metal	N	R_{cut} (\AA)
Li atom	0.06	0.09	0.28	-0.42	1	1.67
(2 \times 2) ML	0.06	0.13	0.22	-0.42 (-0.11)	4	1.48
Na atom	0.05	0.09	0.31	-0.44	1	1.67
(2 \times 2) ML	0.04	0.08	0.23	-0.34 (-0.09)	4	1.61
K atom	0.07	0.09	0.37	-0.53	1	1.72
(2 \times 2) ML	0.06	0.10	0.29	-0.50 (-0.13)	4	1.58
2ML	0.09	0.11	0.28	-0.48 (-0.12/-0.06) [†]	4/8 [†]	1.58
Rb atom	0.07	0.08	0.33	-0.48	1	1.74
(2 \times 2) ML	0.06	0.09	0.34	-0.48 (-0.12)	4	1.62
Cs atom	0.07	0.09	0.35	-0.50	1	1.79
(2 \times 2) ML	0.06	0.09	0.36	-0.52 (-0.13)	4	1.63

[†] There are eight K atoms in two layers, where the lower layer (four atoms) is in a direct contact with the substrate.